Title page for

Perception-based Data Reduction for Haptic Force-feedback Signals using Velocity-adaptive Deadbands

Authors:

Julius Kammerl[1]
Iason Vittorias[2]
Verena Nitsch[3]
Berthold Faerber[3]
Eckehard Steinbach[1]
Sandra Hirche[2]

Affiliation:

[1]Institute for Media Technology (LMT)
[2]Institute of Automatic Control Engineering (LSR)
Technische Universität München, D-80290 Munich, Germany
E-mail: {kammerl,vittorias,eckehard.steinbach}@tum.de, {hirche}@ieee.org

[3]Human Factors Institute (IfA)
University of the Bundeswehr Munich, D-85577 Neubiberg, Germany
E-mail: {verena.nitsch,berthold.faerber}@unibw.de

Corresponding author:

Julius Kammerl
Institute for Media Technology (LMT)
Technische Universität München, D-80290 München
Germany
E-mail: kammerl@tum.de

Perception-based Data Reduction for Haptic Force-feedback Signals using Velocity-adaptive Deadbands

J. Kammerl[1] **I. Vittorias**[2] **V. Nitsch**[3]

B. Faerber[3] **E. Steinbach**[1] **S. Hirche**[2]

[1]Institute for Media Technology (LMT)

[2]Institute of Automatic Control Engineering (LSR)

Technische Universität München, D-80290 Munich, Germany

E-mail: {kammerl,vittorias,eckehard.steinbach}@tum.de, {hirche}@ieee.org

[3]Human Factors Institute (IfA)

University of the Bundeswehr Munich, D-85577 Neubiberg, Germany

E-mail: {verena.nitsch,berthold.faerber}@unibw.de

Abstract

In telepresence and teleaction (TPTA) systems, the transmission of haptic signals puts high demands on the applied signal processing and communication procedures. When running a TPTA session across a packet-based communication network (e.g. Internet), minimizing the end-to-end delay results in packet rates of up to the applied sampling rate of the local control loops at the human system interface and the teleoperator. The

perceptual deadband data reduction approach for haptic signals successfully addresses the challenge of high packet rates in networked TPTA systems and satisfies the strict delay constraints. In this paper, we extend the underlying perceptual model of the deadband approach by incorporating psychophysical findings on human force-feedback discrimination during operators' relative hand movements. By applying velocity-dependent perception thresholds to the deadband approach, we observe further improvement in efficiency and performance due to improved adaption to human haptic perception thresholds. Conducted psychophysical experiments reveal improved data reduction performance of our proposed haptic perceptual coding scheme without impairing the user experience. Our results show a high data reduction ability of up to 96% without affecting system transparency or the operator's task performance.

1 Introduction

Telepresence and teleaction (TPTA) systems allow a human operator to immerse him-/herself into a remote environment by connecting to a remote teleoperator over a communication link. Such systems allow the operator to locally immerse himself into a remote and/or virtual environment that can, for example, be distant, inaccessible, scaled to macro- or nano-dimensions, or hazardous for a human being. They enable the execution of challenging tasks in safety-critical applications, micro assembly, minimally invasive surgery as well as on-orbit telemanipulation tasks in outer space, to name but a few examples. The human operator commands the position/velocity of the teleoperator during the observation of and interaction with the remote environment through multi-modal feedback. The teleoperator itself can be, for instance, a robot equipped with multiple sensors like video-cameras, microphones, as well as force and torque sensors. In order to interact with the remote environment it is equipped with grippers or more anthropomorphic limbs. In case of absolute transparency of the TPTA system, the operator feels as if he was in place of the robot interacting with the environment or in other words, he feels completely

immersed. The quality and performance, in the sense of "degree of immersion", largely rely on the communication of multimodal sensory data exchanged between the operator and the teleoperator. It is well-known that both the operator's immersion into the remote environment as well as the task performance may improve when the operator is provided with visuo-haptic feedback as opposed to visual feedback only (Loeb, 1983; Dennerlein, Martin & Hasser, 2000; Debus, Becker, Dupont, Jang & Howe, 2001; Cockburn & Brewster, 2005; Basdogan, Ho, Srinivasan & Slater, 2000; Tholey, Desai & Castellanos, 2005). In order to enable high-quality operation across rate-limited communication channels between operator and teleoperator (e.g. wireless network in space/underwater TPTA systems), efficient compression schemes for each deployed modality are required. Compression schemes for visual and auditory signals are well-studied topics and a series of widely deployed standards exists. The compression of haptic signals, however, has not been studied extensively yet.

Figure [1] here

As haptic information needs to be sent bidirectionally between the human operator and the teleoperator, the transmitted haptic signals close a global control loop over the communication channel, as shown in Figure 1. Consequently, any time delay in the communication channel can impair the stability of the involved control loops, degrades transparency and reduces task completion time (Wang, Tuer, Rossi, Ni & Shu, 2003; Jay, Glencross & Hubbold, 2007). In order to keep the introduced processing delay in the haptic channel at an absolute minimum, haptic signal updates have to be transmitted immediately. In case of a packet-switched network, e.g. the Internet, this strategy quickly results in high packet rates of up to the typical sampling rate of $1000Hz$, which is required for high-fidelity force feedback and the stability of the local control loops. Due to strict

delay constraints, block-based coding approaches, such as DCT, DWT, Vector Quantization, etc., which are widely used in the field of audio and image/video coding, are not suitable for the compression of haptic signals in TPTA systems.

Depending on the number of degrees of freedom (DOF) and the data type resolution, the typical payload per packet is between 10 and 50 bytes. Taking into account the UDP/IP header overhead of 24 bytes per packet (20 bytes IP, 4 bytes UDP), the overall traffic on the network is considerably increased (50%-100%). The high packet rates of about 1000 packets per second as well as additional data overhead due to the transmission of packet header information become a critical factor (Mahlo, Hoene, Rosami & Wolisz, 2005). Therefore, the reduction of the number of haptic data packets that have to be sent across the network reduces the amount of utilized network resources and is therefore of great benefit.

Early approaches to haptic data compression can be found in Hikichi, Morino, Fukuda, Matsumoto, Yasuda, Arimoto, Iijima & Sezaki (2001) and Shahabi, Ortega & Kolahdouzan (2002), where different sampling and quantization techniques for haptic data are proposed and compared with each other. Applying DPCM and ADPCM with Huffman coding on haptic signals has been proposed in Ortega & Liu (2002) and Borst (2005). Here, the concept of perceptual lossy compression for haptic data has been introduced and the authors propose to adjust the quantization coarseness such that introduced quantization noise stays below absolute human haptic perception thresholds. First lossy compression schemes for haptic data which explicitly incorporate a mathematical model of human haptic perception have been presented in Hinterseer, Steinbach, Hirche & Buss (2005); Hirche, Hinterseer, Steinbach & Buss (2005a,b); Hinterseer & Steinbach (2006) and Hinterseer, Hirche, Chaudhuri, Steinbach & Buss (2008). This so-called perceptual deadband-based data reduction approach (or in short "deadband approach") has been studied in terms of stability criteria in Hirche et al. (2005a,b); Hirche, Hinterseer, Steinbach & Buss (2007); Kuschel, Kremer, Hirche & Buss (2006). The integration of the perceptual model into a lossy compression scheme allows for improved adaption to human

perception thresholds and hence significant data reduction without impairing the perceived quality of the media data. Furthermore, the deadband approach successfully addresses the challenges of high packet rates in the network and strict delay constraints. Based on a simple, yet effective, perceptual model exploiting Weber's Law of Just Noticeable Differences (JND), it allows for signal-adaptive perception-based reduction of haptic samples considered to be relevant for transmission over the communication link. A first theoretical analysis of the performance of the deadband approach appeared in Kammerl, Hinterseer, Chaudhuri & Steinbach (2008). In Hinterseer, Steinbach & Chaudhuri (2006) and Sakr, Zhou, Georganas, Zhao & Shen (2008), the deadband approach is combined with signal prediction and predictive coding in order to further reduce the haptic data rate.

In this article, we propose to extend the deadband coding principle for haptic data reduction by integrating additional psychophysical findings of human haptic perception. Specifically, by exploiting the reduced human force-feedback discrimination ability during simultaneous hand movements of the operator, it is shown that the presented lossy data reduction scheme is capable of further reducing the amount of haptic data on the network without impairing the quality and performance of TPTA systems. Since the efficacy of the traditional Weber-inspired deadband approach with regard to transparent data reduction has been already investigated in previous studies, see e.g. Hirche et al. (2007); Nitsch, Hinterseer, Steinbach, Faerber & Geiger (2008), this article will focus on potential additional benefits of velocity-adaptive perceptual deadbands over the use of the traditional approach.

The remainder of this paper is organized as follows: The Weber-inspired deadband-based data reduction principle is reviewed in Section 2. Section 3 introduces the novel data reduction scheme that is based on velocity-adaptive perceptual deadbands. An experimental study evaluating the proposed approaches is presented in Sections 4. Its results are presented in Section 5 and discussed in Section 6. Section 7 concludes this article.

2 Haptic data reduction using Weber-inspired deadbands

In the following, the deadband-based data reduction principle inspired by Weber's Law of Just Noticeable Differences is discussed.

2.1 Psychophysical Background

In 1834, the experimental physiologist Ernst Weber was among the first to propose a mathematical relationship between the physical intensity of a stimulus and its phenomenologically perceived intensity (Weber, 1851; Gescheider, 1985). Specifically, he proposed the size of the difference threshold (or just noticeable difference, JND) to be a linear function of stimulus intensity. This has become known as Weber's Law of the JND. It can be described by the following implication

$$\frac{\Delta I}{I} = \kappa = constant \tag{1}$$

where I is the stimulus intensity, ΔI is the so-called Difference Threshold or the Just Noticeable Difference (JND) and κ is a constant called the Weber fraction. It describes the smallest amount of change of stimulus intensity I which can be detected just as often as it cannot be detected. In this context, the constant κ describes the linear relationship between the JND and the initial stimulus intensity I. According to Weber's Law, the psychophysical perception of a signal change is therefore proportional to the stimulus intensity itself.

Weber's Law of the JND was found to apply to almost every sense modality, including haptic perception, and over a wide stimulus range (Gescheider, 1985; Tan, Srinivasan, Eberman & Cheng, 1994; Burdea, 1996; Greenspan & Bolanowski, 1996; Allin, Matsuoka & Klatzky, 2002). It allows for the construction of a simple, yet efficient psychophysical model of human haptic perception. Consequently, it can be applied to perceptual coding

schemes, enabling the detection of perceived differences caused by coding artifacts in order to keep them continuously within imperceptible ranges.

2.2 Deadband principle

Inspired by Weber's Law of the JND, we propose to define perceptual deadbands, see Hirche et al. (2007); Hinterseer et al. (2008) and the references therein. They enable the detection of imperceptible changes in the signal, which do not need to be signaled and can be therefore dropped at the encoder.

Figure [2] here

The principle of applying perceptual deadbands for haptic data reduction is shown in Figure 2. Samples illustrated with black circles represent the output of the deadband data reduction scheme. They define perception thresholds represented by a deadband, illustrated as gray zones. Please note that the size of the applied deadband Δ_i at discrete time i is a function of a deadband parameter k and the signal amplitude of the recently transmitted force-feedback sample value f_{i-m}, where m samples back in time the last perception threshold violation took place. By this means, the deadband parameter k closely relates to the Weber threshold parameter κ. It can be described by

$$\Delta_i = \Delta_{i-1} = \cdots = \Delta_{i-m} = k \cdot |f_{i-m}|. \tag{2}$$

Once the deadband is violated by a new input sample, this input sample is considered to be relevant for encoding/transmission and redefines the applied perception thresholds. Samples with blank circles fall within the currently defined deadband and can be dropped as their change in signal is too small to be perceptible. As only the samples which violate

the deadband are considered to contain perceptible information, the deadband-based data reduction scheme allows for signal-adaptive downsampling and therefore significantly reduces the amount of samples within the haptic data streams. In case of noisy sensors, a minimum absolute deadband size exceeding the current noise level should be defined.

2.3 Decoding of deadband encoded signals & stability issues

The deadband approach adaptively samples haptic signals in order to reduce the amount of network packets on the communication channel. However, local control loops at the HSI and the teleoperator require a constant and high sampling rate. Consequently, the irregularly received signal updates need to be upsampled to a constant sample rate again. Hinterseer et al. (2005) proposes to use a simple zero-order hold (ZOH) strategy. Clocked by the desired output sampling rate, it holds and replicates the most recently received sample until a new signal sample updates its internal state. One main advantage of the ZOH reconstruction method is that the desired signal upsampling can be achieved without adding any additional algorithmic delay to the signal.

However, as it was shown in Adams & Hannaford (1999), this ZOH reconstruction strategy is non-passive due to a nonzero phase lag for $0 < \omega < \frac{2\pi}{T}$, where T is the sampling interval. As the signal behavior is not known in advance, there is a chance of energy generation associated with potential destabilization of the system. In order to assure control loop stability, Hirche et al. (2005b, 2007) propose to satisfy this requirement by implementing a modified hold-last-sample reconstruction strategy for deadband encoded signals. By assuring that the mechanical power of the reconstructed signals is always less than the input mechanical power, passivity, and thus stability, is guaranteed. In case of energy generation due to signal reconstruction, the ZOH reconstruction algorithm is switched to a more conservative, energy dissipating mode, which reconstructs modified output signals with reduced energy that are still in compliance within the applied perception thresholds. Note, however, that passivity is only a sufficient condition, i.e., a non-passive system is not

necessarily unstable. In particular, if the system damping is high enough, slightly non-passive behavior of the reconstruction strategy can be accommodated without losing stability. This explains why we could employ a simple ZOH strategy in our experiments without experiencing stability problems. Furthermore, the controller at the teleoperator and the HSI as well as the communication channel are implemented in discrete time. It is well-known that the passivity property in the system can be lost during the sampling step (Colgate & Schenkel, 1997). However, in typical TPTA systems, where the local controller sampling rate is 1 kHz and more, these sampling effects are considered negligible.

3 Data reduction using velocity dependent adaptive deadbands

Weber's law infers perceptual limits of the human haptic modality; however, very few of the empirical studies which investigate these limits consider the effects of dynamic movements and attentional requirements, both of which are important aspects of real-life task performance. Based on this rationale, we propose to extend the previously discussed Weber-inspired deadband-based data reduction principle by incorporating an additional perceptual dimension, namely the velocity of the operator's hand movement.

3.1 Psychophysical background

Whilst several studies suggest that haptic perceptive abilities are superior with active as opposed to passive movements (Heller, Roger & Perry, 1990; Symmons, Richardson & Wuillemin, 2004), attentional theories suggest that the opposite occurs when attention is divided between several goals or directed towards a specific task; see Eysenck & Keane (2000) for an overview. For example, in a realistic TPTA-based scenario, an operator would be required to plan, control and execute certain movements. These movements usually need to be executed with some degree of precision, in terms of position as well as force, in order to achieve a task objective. In this case one would speculate that less cognitive resources are available to devote attention to the perception and interpretation of

the force feedback received, in particular, if these force signals, or a distortion thereof, are not strictly task-relevant. Thus, it would seem likely that task-directed movement reduces the operator's ability to perceive changes in displayed force-feedback, thus increasing JNDs between stimuli.

Although literature on this topic is scarce, empirical evidence seems to support this assumption. Several studies suggest that attention may have a direct effect on human haptic perceptive ability by triggering a remodulation of neuronal activity in the primary sensory cortex (Iguchi, Hoshi & Hashimoto, 2001; Braun, Haug, Wiech, Birbaumer, Elbert & Roberts, 2002). Other studies found direct support for increased JNDs in the presence of multiple attentional demands. For example, Wright, Green & Baker (2000) found in a study on change blindness, that the log of the Weber parameter is proportional to the log of the number of targets given. Moreover, Yang, Bischof & Boulanger (2008) found that force discrimination thresholds were greater during hand movements than they were reported by studies in which no hand movement occurred. This effect was independent of the speed of movement. Zadeh, Wang & Kubica (2008) analyzed the influence of hand movements on absolute force perception thresholds (AFT) in the context of haptic data reduction. They found AFTs to increase when the operator's hand is in motion. However, neither difference detection thresholds nor performance and/or efficiency of corresponding data reduction architectures were investigated in their work.

3.2 Velocity-adaptive deadband principle

Aiming to adjust the deadband data reduction approach to the demands of real-life TPTA-applications, we propose to modify the deadband approach with respect to the operator's hand velocity, thus exploiting the potentially increased JNDs during task-directed hand movement for the purpose of increased, yet still imperceptible, data reduction. Specifically, we model the deadband parameter as a function of velocity

$$\phi = k + \alpha \cdot |\dot{x}| \tag{3}$$

where the velocity-adaptive deadband parameter ϕ is determined by the sum of the constant component k and a velocity-proportional component characterized by the factor $\alpha \geq 0$. The parameter k represents a velocity-independent component of the JND. Adjusting α allows us to control the influence of the velocity on the resulting modified deadband parameter ϕ. For $\alpha = 0$ the velocity independent relationship in (1) is obtained.

Figure [3] here

Accordingly, the size of the applied deadband bounds becomes

$$\begin{aligned} \Delta_i &= \phi \cdot |f_{i-m}| \\ &= (k + \alpha \cdot |\dot{x}_i|) \cdot |f_{i-m}| \end{aligned} \tag{4}$$

where the last violation of the deadband occurred at time $i - m$.

An example of the applied adaptive deadband parameter ϕ recorded during the experimental evaluation in Section 4 is shown in Figure 3. The velocity signal $\dot{x}$ referring to the operator's hand movements is illustrated in Figure 3(a). It is used to define the velocity-adaptive deadband parameter ϕ, shown in Figure 3(b).

3.3 System architecture

Figure [4] here

The architecture of our proposed velocity-adaptive deadband-based data reduction scheme is illustrated in Figure 4, where $\dot{x}_h$ and f_h denote the velocity and the force-feedback signal on the human operator side, respectively; $\dot{x}_t$ denotes the velocity of the teleoperator and f_e represents the environment force. The HSI measures the human operator's hand movements and corresponding motion commands are sent across the network at high rate in order to control the teleoperator. In this work, the focus is on the evaluation of our proposed velocity-adaptive deadband scheme and therefore it was applied only on the force channel; no data reduction was applied on the velocity channel. However, our previously developed schemes can be applied on the velocity transmitting forward channel in order to achieve bilateral haptic data reduction in the system (Hinterseer et al., 2008).

At the teleoperator, the received velocity information enters the novel adaptive deadband block modifying the current deadband size according to (4). Compared with the data reduction principle discussed in Section 2, larger deadbands can be applied during movements of the operator's hand. A change in the force-feedback signal is only transmitted in case the applied perception threshold is violated. Thereby, an additional reduction in packet rate on the communication channel can be achieved.

4 Experimental Evaluation

To evaluate whether the velocity-dependent deadband coding scheme constitutes an improvement to the traditional Weber-inspired approach in terms of transparent, i.e. imperceptible, data reduction, an experimental study has been conducted. Firstly, it was aimed to determine the respective disturbance detection thresholds of the coding parameters, e.g., the constant component k, basis of the traditional Weber-inspired deadband approach, as well as the velocity adaptation parameter α from (4), which forms the basis of the proposed velocity-adaptive deadband extension. Secondly, it was to be tested whether either factor changed significantly with the speed of the movement performed by participants. Finally, it was to be investigated whether incorporating the

velocity adaptation parameter α into the Weber-inspired deadband data reduction approach would lead to a significant packet rate reduction without adversely affecting the accuracy of teleoperator control.

4.1 Participants

18 male and 3 female students participated in the experiment (mean age = 27 years, std. deviation = 2.5 years), all of whom were right-handed and naive to the purpose of the experiment and the experimental setup. One person's data set had to be excluded from further analysis due to measurement irregularities.

4.2 Apparatus

The experimental testbed consisted of a tubular linear motor, Thrusttube 2510 from Copley Controls Corp., shown in Figure 5(a), a Burster Corp. 8524-5500 force sensor and two PCs. The linear motor was able to display peak forces of up to 780 N and continuous stall forces of up to 104.3 N and was connected to a digital servo drive Xenus XTL, also from Copley Controls Corp. The digital servo operated in current control; thus, we can consider the signal input to be approximately proportional to the applied motor force. The position was measured by an optical incremental encoder with a precision of 1 μm. The force sensor had a measurement range of 0 ± 500 N with an accuracy of 0.25% in full scale. The entire haptic interface was controlled by a PC running a real-time Linux operating system. The digital servo was connected to the PC through a Sensoray I/O card. The overall haptic device was controlled by a high-gained force controller which compensated for viscous and Coulomb friction as well as for external forces. This resulted in reduced device dynamics displayed to the human, i.e. 0.35 kg inertia and 3.01 Ns/m damping that were considered negligible for the purpose of the experiment. For the virtual environment, a virtual spring was chosen supported by the fact that the mechanical spring represents a generic and simple design of many environments on haptic tasks. It acted as an

admittance, namely received velocity information from and provided force feedback to the device. All the control functions were implemented by Simulink blocksets. The sampling rate of the haptic signals and the local control loops was 1 kHz. A second PC, also running a real-time Linux kernel, received position information in order to visualize a virtual teleoperator within a virtual telepresence environment. The connection between the two PCs was UDP/IP-based and time delay was on average less than 1 ms and was considered to be negligible. Two potentiometers enabled participants to control the parameters k and α online and allowed for adjustments of k and α to maximum settings of 0.40 and 1.20, respectively, with a resolution of 0.01.

Figure [5] here

4.3 Experimental design

The study made use of a 2 (deadband type) x 3 (motion speed) within-subjects design. In order to introduce a measure of task performance accuracy and to ensure that participants move the master device with similar motion speeds, participants were given a task. Task objective was to control the movement of the virtual teleoperator so as to follow a moving cursor as closely as possible whilst participants experienced force-feedback originating from a virtual spring which covered the entire motion range on both directions. The spring constant was set to 100 N/m during all experiments. Assuming the users followed the cursor perfectly a maximum displacement of 15 cm was measured resulting in 15 N of maximum intended force. A screenshot of the visual feedback is illustrated in Figure 5(b). The motion speed with which the cursor moved from one side of the computer screen to the other was manipulated in a sinusoidal manner using three different frequencies: low, medium and high (2, 3 and 4 rad/sec). The maximum for each motion speed level was 0.12

m/sec, 0.18 m/sec and 0.24 m/sec. During the experiment, preferable configuration settings for the force component k, and for the velocity adaptation parameter α were measured for each speed. Also measured for each speed of movement were the resulting mean squared error (mse) of the distance between computer cursor and teleoperator positions including the data packet rates with use of the two deadband schemes.

4.4 Procedure

Participants were first demonstrated the effects of the component k as well as the velocity adaptation parameter α on the quality of the displayed force feedback signal; and they were given the opportunity to familiarize themselves with the task, the potentiometers and their effects on the control of the teleoperator. A carefully designed training phase ensured that all participants were approximately at the same level of training, as far as the detection of possible signal disturbances is concerned. They were then asked to continuously perform the task of following the moving cursor as closely as possible using the haptic device and the cursor coupled to it. In our experiment, an adapted method of adjustment was used for detecting and measuring absolute thresholds that allowed us to test a wide range of parameter values, see e.g. Gescheider (1985). Whilst performing the task, participants were to adjust the parameters k and α, using the potentiometers, until they found the maximum setting with which no disturbance was felt. This disturbance would manifest itself in the form of increasingly abrupt dislocations of the force feedback device, which in turn required greater physical effort to precisely control the position of the teleoperator. All participants were instructed to use the same strategy for finding this setting, that is, to alternate between settings that lie below and above the perceived threshold. Specifically, they were asked to approach the target setting from both directions, i.e., initially starting to slowly increase from the minimum parameter value, followed by slowly decreasing from a maximum value, until they were confident that they had found the highest setting at which they felt no disturbance in the control of the teleoperator. In

a first step, participants focused on finding an optimum configuration for k starting with its lowest setting ($k = 0$) while the velocity adaptation parameter α was set to zero. When they were confident that they had found the target setting, performance was measured for 10 seconds using the setting that participants had adjusted to. During these 10 seconds, participants only focused on their task performance. This procedure was repeated to find an optimum velocity adaptation parameter α with k still set to the participants' preferred configuration. Afterwards, both steps were repeated with two other speeds of movement.

The order of the three speed conditions, which determined the speed of the computer cursor, and consequently participants' hand movements, was systematically randomized for each participant. Participants were also given headphones which prevented them from hearing sounds that might distract or influence them in any way. In addition, all participants were instructed to use the same type of grip, i.e., a heavy wrap grip as classified by Cutkosky & Howe (1990), on the master device.

5 Results

Data were inspected for outliers, as well as for normality and homogeneity of variance. Data with z-scores of $z > \pm 3.29$ were excluded from further analysis. Where a violation of the assumptions of parametric data was suspected, necessary corrections have been made, as specified below.

5.1 Disturbance detection thresholds for k and α

The mean settings and standard deviations for parameters k and α that participants adjusted to for each movement speed without feeling any introduced coding artifacts are displayed in Table 1.

The presented results indicate that the mean preferred setting for the constant component k lies at around 0.06. The mean preferred value for the velocity adaptation parameter α has been detected to be approximately 0.15.

Guided speed	Parameter $\boldsymbol{k}$		Parameter $\boldsymbol{\alpha}$	
	mean	std. deviation	mean	std. deviation
low	0.053	0.053	0.15	0.11
medium	0.064	0.056	0.15	0.10
high	0.059	0.027	0.16	0.13

Table 1: Preferred configuration for the parameters k and α of the adaptive deadband coding scheme with respect to different speed levels. Maximum settings possible were 0.40 and 1.20 for k and α, respectively.

5.2 Velocity dependency of parameters k and α

In order to determine the influence of the velocity of the operator's hand on the respective deadband detection thresholds for the Weber-inspired and velocity-adaptive deadband types, as indicated by k and α, two within-subjects univariate analyses of variance (ANOVA) were conducted with hand movement speed as independent variable and adjusted k and α settings as dependent variables, respectively. Since Mauchley's test of sphericity was significant
($\chi^2(2) = 9.74, p < 0.05$), F-values for factor k were adjusted using Greenhouse-Geisser corrections ($\epsilon = 0.71$). The ANOVA showed that neither k ($F(1.41, 26.80) = 0.58, p = 0.57$) nor α ($F(2, 38) = 0.08, p = 0.93$) varied significantly with motion speed. This suggests that the effects of each component are velocity independent. That is, participants adjusted to very similar values for k and α, regardless of the speed at which they performed their movement. While the number of participants in this study would not suffice to detect small effects of speed on k and α values, the results provide an indication that the design and the deployed psychophysical function consisting of a constant component k and a velocity-proportional component characterized by α is a valid assumption.

5.3 Effects of parameters k and α on operator task performance and data reduction performance

Figure [6] here

In order to determine whether or not the use of velocity-adaptive deadbands achieves greater data reduction compared to the Weber-inspired approach without deteriorating performance accuracy, two further repeated-measures ANOVA were conducted with movement speed (low, medium, high) and deadband type (non-adaptive vs. adaptive) as independent variables, and task performance accuracy (mean squared position error) as well as data reduction performance (signal updates per second) as dependent variables, respectively.

With regard to data reduction performance, F-values for speed effects were adjusted using Greenhouse-Geisser corrections ($\epsilon = 0.68$) as Mauchley's test of sphericity was significant ($\chi^2(2) = 11.83, p < 0.05$). Despite a trend of increasing signal updates with increasing motion speed as indicated by the mean values, the ANOVA did not find a significant main effect of speed on data reduction performance ($F(1.35, 25.65) = 0.57$, $p = 0.51$). However, it did reveal a significant main effect of deadband type ($F(1, 19) = 18.43$, $p < 0.001$, part. $\eta^2 = 0.49$). The interaction between motion speed and deadband type was not significant ($F(2, 38) = 0.03$, $p = 0.98$). Looking at the mean values, the results indicate that the use of adaptive deadbands significantly reduced the number of signal updates performed per second, see Figure 6(a), regardless of the speed at which participants moved their hands.

For the ANOVA of task performance data, F-values for speed effects were adjusted using Greenhouse-Geisser corrections ($\epsilon = 0.62$) as Mauchley's test of sphericity was significant ($\chi^2(2) = 16.60, p < 0.05$). The ANOVA revealed a significant main effect of speed on mean squared position error ($F(1.25, 23.71) = 32.59$, $p < 0.001$, part. $\eta^2 = 0.63$). Not

surprisingly, Bonferroni-adjusted post-hoc comparisons indicated that the mean squared position error increased significantly with higher levels of velocity (low vs. medium $F(1, 19) = 32.32$, $p < 0.001$, part. $\eta^2 = 0.63$; medium vs. high $F(1, 19) = 13.34$, $p < 0.01$, part. $\eta^2 = 0.41$), as indicated by the mean values illustrated in Figure 6(b). However, there was no significant main effect of deadband type on position error ($F(1, 19) = 0.04$, $p = 0.85$), suggesting that task performance accuracy did not significantly deteriorate with the use of velocity-adaptive deadbands compared to the use of nonadaptive deadbands.

The mean values of the respective packet rates for each velocity showed that the adaptive deadband approach led to significantly greater data reduction compared to the Weber-inspired deadband coding scheme, as shown in Figure 6(a).

6 Discussion

The main contribution of this work is a novel data reduction approach for haptic signals with deadbands that dynamically change, aiming to exploit human haptic perception and discrimination limitations during task-directed hand movements. It is inspired by Weber's Law of the JND and assumes the deadband size to be a linear function of the velocity of the human operator's hand movement.

Psychophysical experiments were conducted aiming to assess whether or not the proposed perceptual coding scheme can be considered superior to the traditional deadband approach in terms of transparent data reduction.

The results indicate an optimum configuration of approximately $k = 0.06$ and $\alpha = 0.15$, regardless of the speed at which participants operated the master device. These settings indicate the average deadband detection threshold, defined as the maximum setting at which no disturbance is felt by the participants. It should be kept in mind that, since participants were motivated to find settings that lie below the disturbance threshold, these settings are likely to reflect a conservative response tendency. Thus there remains a

possibility that even greater data reduction may be used without a noticeable deterioration in performance accuracy or signal quality. On the other hand, one must also consider that the present study was only designed to test for large effects. Using a substantially larger participant pool might find small deteriorative effects. Nevertheless, considering the fine resolution of the potentiometers combined with the fact that participants optimum settings confine themselves to a fairly narrow range of the entire spectrum possible, see Table 1, the results presented in this study appear to represent a fairly accurate approximation to participants' subjective experiences.

Overall, the results suggest that the velocity-adaptive deadband approach constitutes a significant improvement to the traditional Weber-inspired deadband approach in terms of data reduction performance. In our experiment, adding the velocity-proportional component controlled by α to the constant component k led to further significant reduction in sent data packets, thus allowing for an additional data reduction of up to 30% compared to the Weber-inspired deadband approach (total data reduction of 96%), without perceptibly impairing the quality of the force-feedback signal or significantly affecting task performance accuracy. Since this effect was observed for all three motion speeds tested, the concept of the velocity-dependent data reduction approach seems to be valid.

It should be pointed out that, whilst the adaptive deadband approach is certainly inspired by traditional psychophysical models and draws on findings of cognitive and neuropsychological studies, the present study was neither designed nor destined to make any substantiated claims regarding the role of directed attention in force perception. As such, it provides further impetus for future studies to examine the role of cognition in human haptic perception.

7 Conclusion

The present paper proposes a modification to a haptic data reduction approach which aims to exploit dynamic human haptic perception limitations. An evaluative study found this

modification to be a significant improvement to the traditional deadband-based data reduction approach, as it achieved even greater data reduction without significantly affecting task performance. Future studies are planned to investigate additional psychophysical factors influencing human force-feedback perception which may be exploited for data reduction purposes, such as the direction of force stimuli. It is also intended to extend the presented coding scheme for teleoperation architectures to time-delayed scenarios, such as the so-called scattering transformation. Moreover, the role of task context and hardware components in the use of velocity-dependent deadband needs to be systematically investigated in order to ascertain the extent of generalizability of our results to other TPTA systems and scenarios.

Acknowledgment

The authors would like to thank the anonymous reviewers for their valuable comments and suggestions. This work was supported by the German Research Foundation (DFG) within the Collaborative Research Centre SFB 453 on "High-Fidelity Telepresence and Teleaction".

References

Adams, R. & Hannaford, B. (1999). Stable haptic interaction with virtual environments. *IEEE Transactions on Robotics and Automation*, *15*(3), 465–474.

Allin, S., Matsuoka, Y., & Klatzky, R. (2002). Measuring just noticeable differences for haptic force feedback: implications for rehabilitation. In *Proceedings of the 10th Symposium on Haptic Interfaces for Virtual Environment and Teleoperator Systems*, (pp. 299–302)., Orlando, FL, USA.

Basdogan, C., Ho, C.-H., Srinivasan, M. A., & Slater, M. (2000). An experimental study on the role of touch in shared virtual environments. *ACM Transactions on Human Computer Interaction TOCHI*, *7*(4), 1–14.

Borst, C. (2005). Predictive coding for efficient host-device communication in a pneumatic force-feedback display. In *Proceedings of the First Joint Eurohaptics Conference and Symposium on Haptic Interfaces for Virtual Environment and Teleoperator Systems, World Haptics*, (pp. 596–599)., Pisa, Italy.

Braun, C., Haug, M., Wiech, K., Birbaumer, N., Elbert, T., & Roberts, L. (2002). Functional organization of primary somatosensory cortex depends on the focus of attention. *Neuroimage*, *17*, 1451–1458.

Burdea, G. C. (1996). *Force and Touch Feedback for Virtual Reality*. Wiley.

Cockburn, A. & Brewster, S. (2005). Multimodal feedback for the acquisition of small targets. *Ergonomics*, *48*(9), 1129–1150.

Colgate, E. & Schenkel, G. (1997). Passivity of a class of sampled-data systems: Application to haptic interfaces. *Robotic Systems*, *14*, 37–47.

Cutkosky, M. & Howe, R. (1990). Human grasp choice and robotic grasp analysis. In *Dextrous robot hands* (pp. 5–31). NewYork:Springer.

Debus, T., Becker, T., Dupont, P., Jang, T., & Howe, R. (2001). Multichannel vibrotactile display for sensory substitution during teleoperation. In *Proceedings of the SPIE - The International Society for Optical Engineering*, (pp. 42–49)., Newton, MA, USA.

Dennerlein, J., Martin, D., & Hasser, C. (2000). Force-feedback improves performance for steering and combined steering-targeting tasks. In *Proceedings of the SIGCHI conference on Human factors in computing systems*, (pp. 423–429)., The Hague, The Netherlands.

Eysenck, M. W. & Keane, M. T. (2000). *Cognitive Psychology. A student's handbook*. Psychology Press.

Gescheider, G. A. (1985). *Psychophysics*. Lawrence Erlbaum.

Greenspan, J. & Bolanowski, S. (1996). *The Psychophysics of Tactile Perception and Its Peripheral Physiological Basis, In: L. Kruger (Ed.). Pain and Touch*. Academic Press Inc.

Heller, M. A., Roger, G., & Perry, C. (1990). Tactile pattern recognition with the optacon: Superior performance with active touch and the left hand. *Neuropsychologia*, *28*, 1003–1006.

Hikichi, K., Morino, H., Fukuda, I., Matsumoto, S., Yasuda, Y., Arimoto, I., Iijima, M., & Sezaki, K. (2001). Architecture of haptics communication system for adaptation to network environments. In *Proceedings of the IEEE International Conference on Multimedia and Expo*, (pp. 563–566)., Tokyo, Japan.

Hinterseer, P., Hirche, S., Chaudhuri, S., Steinbach, E., & Buss, M. (2008). Perception-based data reduction and transmission of haptic data in telepresence and teleaction systems. *IEEE Transactions on Signal Processing*, *56*(2), 588–597.

Hinterseer, P. & Steinbach, E. (2006). A psychophysically motivated compression approach for 3d haptic data. In *Proceedings if the 14th Symposium on Haptic Interfaces for Virtual Environment and Teleoperator Systems*, (pp. 35–41)., Arlington, VA, USA.

Hinterseer, P., Steinbach, E., & Chaudhuri, S. (2006). Model based data compression for 3d virtual haptic teleinteraction. In *International Conference on Consumer Electronics, ICCE. Digest of Technical Papers.*, (pp. 23–24)., Las Vegas, USA.

Hinterseer, P., Steinbach, E., Hirche, S., & Buss, M. (2005). A novel, psychophysically motivated transmission approach for haptic data streams in telepresence and teleaction systems. In *Proceedings of the International Conference on Acoustics, Speech, and Signal Processing*, volume 2, (pp. ii/1097–ii/1100)., Philadelphia, USA.

Hirche, S., Hinterseer, P., Steinbach, E., & Buss, M. (2005a). Network traffic reduction in haptic telepresence systems by deadband control. In *Proceedings of the IFAC World Congress, International Federation of Automatic Control*, Prague, Czech Republic.

Hirche, S., Hinterseer, P., Steinbach, E., & Buss, M. (2005b). Towards deadband control in networked teleoperation systems. In *Proceedings of the IFAC World Congress, International Federation of Automatic Control*, Prague, Czech Republic.

Hirche, S., Hinterseer, P., Steinbach, E., & Buss, M. (2007). Transparent data reduction in networked telepresence and teleaction systems. part i: Communication without time delay. *Presence: Teleoperators & Virtual Environments*, *16*(5), 523–531.

Iguchi, Y., Hoshi, Y., & Hashimoto, I. (2001). Selective spatial attention induces short-term plasticity in human somatosensory cortex. *Neuroreport*, *12*, 3133–3136.

Jay, C., Glencross, M., & Hubbold, R. (2007). Modeling the effects of delayed haptic and visual feedback in a collaborative virtual environment. *ACM Transactions on Computer-Human Interaction*, *14*(2), 8/1–31.

Kammerl, J., Hinterseer, P., Chaudhuri, S., & Steinbach, E. (2008). A theoretical analysis of data reduction using the weber quantizer. In *Proceedings of the International Data Compression Conference, DCC*, (pp. 524–524)., Snowbird, UT, USA.

Kuschel, M., Kremer, P., Hirche, S., & Buss, M. (2006). Lossy data reduction methods for haptic telepresence systems. In *Proceedings of the International Conference on Robotics and Automation*, (pp. 2933–2938)., Orlando, Florida, USA.

Loeb, K. (1983). Membrane keyboards and human performance. *The Bell System Technical Journal*, *26*, 1733–1749.

Mahlo, C., Hoene, C., Rosami, A., & Wolisz, A. (2005). Adaptive coding and packet rates for tcp-friendly voip flows. In *Proceedings of the 3rd International Symposium on Telecommunications*, Shiraz, Iran.

Nitsch, V., Hinterseer, P., Steinbach, E., Faerber, B., & Geiger, L. (2008). An experimental study of lossy compression in a real telepresence and teleaction system. In *Proceedings of the IEEE International Workshop on Haptic Audio Visual Environments*, (pp. 75–80)., Ottawa, Canada.

Ortega, A. & Liu, Y. (2002). Lossy compression of haptic data. In *Touch in Virtual Environments: Haptics and the Design of Interactive Systems* chapter 6, (pp. 119–136). Prentice Hall.

Sakr, N., Zhou, J., Georganas, N., Zhao, J., & Shen, X. (2008). Prediction-based haptic data reduction and compression in tele-mentoring systems. In *IEEE Proceedings on Instrumentation and Measurement Technology Conference*, (pp. 1828–1832)., Austin, Texas, USA.

Shahabi, C., Ortega, A., & Kolahdouzan, M. R. (2002). A comparison of different haptic compression techniques. In *Proceedings of the International Conference on Multimedia & Expo*, (pp. 657–660)., Lausanne, Switzerland.

Symmons, M. A., Richardson, B., & Wuillemin, D. (2004). Active versus passive touch: superiority depends more on the task than the mode. In *Touch, Blindness, and Neuroscience* (pp. 179–185). UNED.

Tan, H., Srinivasan, M., Eberman, B., & Cheng, B. (1994). Human Factors for the Design of Force-Reflecting Haptic Interfaces. *Tan, Srinivasan, Eberman, & Chang, ASME WAM*, 1–11.

Tholey, G., Desai, J., & Castellanos, A. (2005). Force feedback plays a significant role in minimally invasive surgery. *Annals of Surgery*, *241*(1), 102–109.

Wang, D., Tuer, K., Rossi, M., Ni, L., & Shu, J. (2003). The effect of time delays on tele-haptics. In *Proceedings of the 2nd IEEE International Workshop on Haptic, Audio and Visual Environments and Their Applications*, (pp. 7–12)., Ottawa, Ontario, Canada.

Weber, E. H. (1851). *Die Lehre vom Tastsinn und Gemeingefuehl, auf Versuche gegruendet.* Vieweg: Braunschweig, Germany.

Wright, M., Green, A., & Baker, S. (2000). Limitations for change detection in multiple garbor targets. *Visual Cognition*, *7*, 237–252.

Yang, X.-D., Bischof, W., & Boulanger, P. (2008). Perception of haptic force magnitude during hand movements. In *Proceedings of the International Conference on Robotics and Automation*, (pp. 2061–2066)., Pasadena, CA, USA.

Zadeh, M. H., Wang, D., & Kubica, E. (2008). Perception-based lossy haptic compression considerations for velocity-based interactions. *Multimedia Systems*, *13*, 275–282.

FIGURE 1

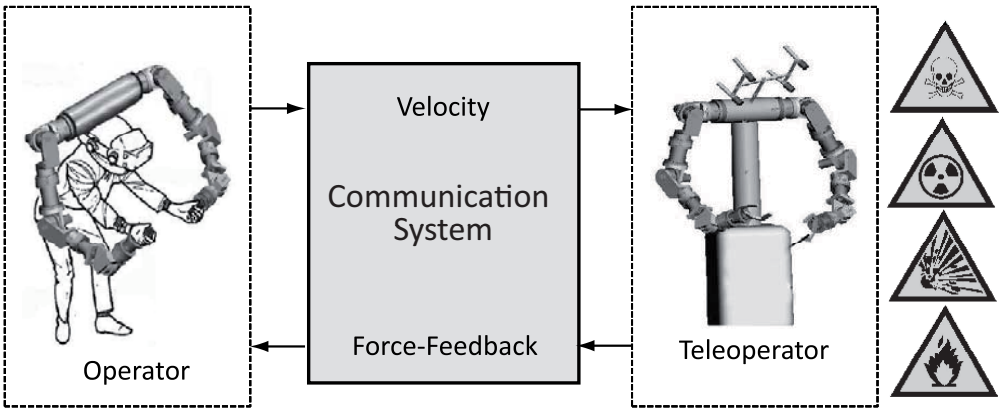

Figure 1: Overview of haptic communication in a telepresence and teleaction system.

Size: **One column**

FIGURE 2

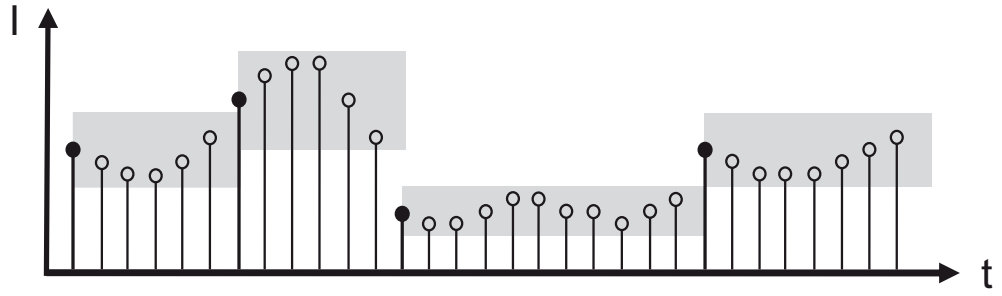

Figure 2: Principle of deadband-based data reduction.

Size: **One column**

FIGURE 3

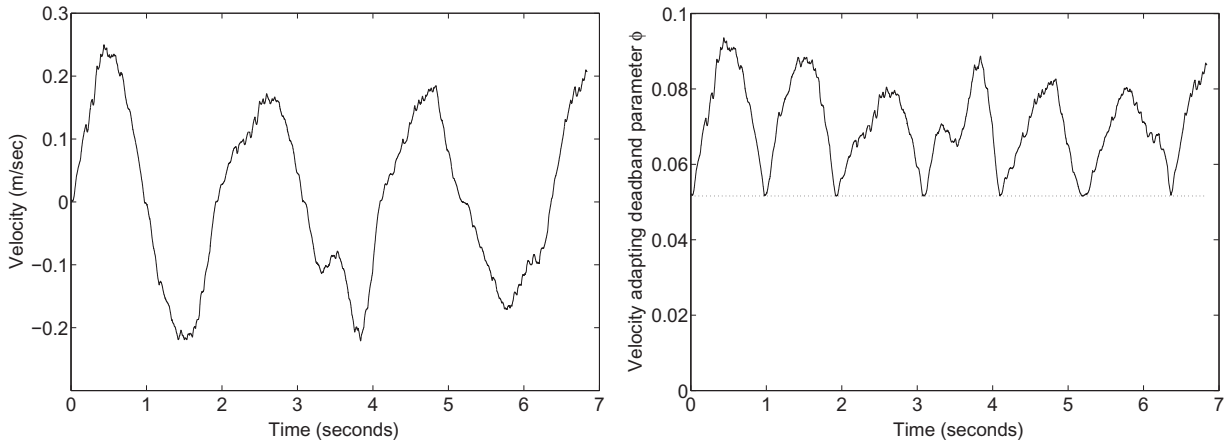

(a) Velocity signal $\dot{x}$ tracked by the HSI

(b) Corresponding ϕ for $\alpha = 0.16$ and $k = 0.05$

Figure 3: Adaptive deadband parameter ϕ as a function of velocity.

Size: **Two columns**

FIGURE 4

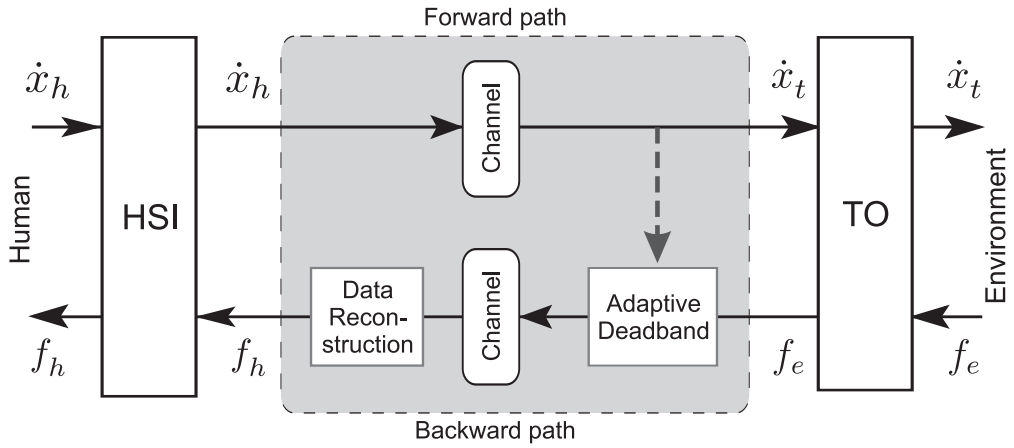

Figure 4: Architecture of the adaptive deadband data reduction principle. The size of the applied deadband adapts to the velocity signal $\dot{x}$.

Size: **One column**

FIGURE 5

(a) Tubular linear motor, Thrusttube 2510

(b) Simulated visual feedback

Figure 5: Illustration of the experimental testbed. The left Figure 5(a) shows the deployed HSI device where subjects experience force-feedback from a virtual spring. The right Figure 5(b) shows a virtual teleoperator environment.

Size: **Two columns**

FIGURE 6

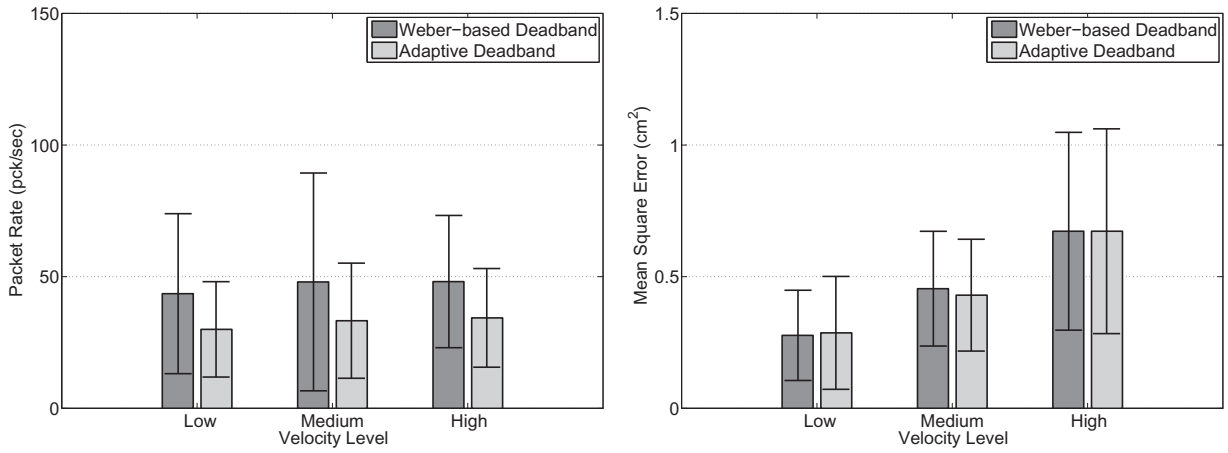

(a) Mean packet rates

(b) Task performance accuracy

Figure 6: Mean values and standard deviations of packet rates and performance results with respect to velocity level and deadband type. The dark bars show results for the Weber-inspired (non-adaptive) deadband approach described in Section 2. The light bars represent results for the proposed novel velocity-adaptive deadband data reduction scheme. Compared to Weber-inspired deadbands, an additional mean packet rate reduction of 30.1% without effects on task performance accuracy is achieved when using velocity-dependent deadbands.

Size: **Two columns**

Figure captions:

Figure 1: Overview of haptic communication in a telepresence and teleaction system.

Figure 2: Principle of deadband-based data reduction.

Figure 3: Adaptive deadband parameter ϕ as a function of velocity.

(a) Velocity signal $\dot{x}$ tracked by the HSI.

(b) Corresponding ϕ for $\alpha = 0.16$ and $k = 0.05$.

Figure 4: Architecture of the adaptive deadband data reduction principle. The size of the applied deadband adapts to the velocity signal $\dot{x}$.

Figure 5: Illustration of the experimental testbed. The left Figure 5(a) shows the deployed HSI device where subjects experience force-feedback from a virtual spring. The right Figure 5(b) shows a virtual teleoperator environment.

(a) Tubular linear motor, Thrusttube 2510

(b) Simulated visual feedback

Figure 6: Mean values and standard deviations of packet rates and performance results with respect to velocity level and deadband type. The dark bars show results for the Weber-inspired (non-adaptive) deadband approach described in Section 2. The light bars represent results for the proposed novel velocity-adaptive deadband data reduction scheme. Compared to Weber-inspired deadbands, an additional mean packet rate reduction of 30.1% without effects on task performance accuracy is achieved when using velocity-dependent deadbands.

(a) Mean packet rates

(b) Task performance accuracy